

Parameter estimation in the presence of the most general Gaussian dissipative reservoir

Marcin Jarzyna* and Marcin Zwierz†

Faculty of Physics, University of Warsaw, ulica Pasteura 5, PL-02-093 Warszawa, Poland

(Dated: 21st October 2018)

We analyze the performance of quantum parameter estimation in the presence of the most general Gaussian dissipative reservoir. We derive lower bounds on the precision of phase estimation and a closely related problem of frequency estimation. For both problems we show that it is impossible to achieve the Heisenberg limit asymptotically in the presence of such a reservoir. However, we also find that for any fixed number of probes used in the setup there exists a Gaussian dissipative reservoir, which, in principle, allows for the Heisenberg-limited performance for that number of probes. We discuss a realistic implementation of a frequency estimation scheme in the presence of a Gaussian dissipative reservoir in a cavity system.

PACS numbers: 03.65.Ta, 06.20.-f, 42.50.-p, 42.50.Lc

I. INTRODUCTION

The ability to perform precise measurements of physical quantities is of utmost importance to all branches of science. An example of this is a recent spectacular detection of gravitational waves by interferometric techniques [1, 2]. The precision of all realistic measurement setups is limited by various errors caused by detection imperfections and noise present in the setup. Because of this the state-of-the-art experiments are performed in such a way as to decrease the impact of all sources of experimental errors, both the systematic and the statistical ones. This is done by carefully designing all stages of the experiment and, more importantly, by actively screening the experimental setup from the surrounding noise. Strikingly, however, no matter how much effort we put into our design there is always a physical limitation to any such procedure, as nature itself sets limits on precision via the principles of quantum mechanics [3].

In most cases, we express the precision limits in terms of the energy, or equivalently, the average number of probes \bar{N} used in the experiment as all realistic measurement schemes have to operate on limited resources. This is because either the power of our source is limited or the experimental scheme has an upper limit on the energy that it can sustain [4, 5]. Typically, the higher the number of probes, hence the energy used, the better is the precision. In the classical regime, the probes are independent from each other and the precision is bounded by a standard quantum limit (SQL) or the shot noise scaling $1/\sqrt{\bar{N}}$. On the other hand, using quantum

features of nature, such as entanglement we can reduce the estimation error and thus improve the precision. In the general case of parameter estimation, the ultimate bound set by quantum physics is the so-called Heisenberg limit $1/\bar{N}$ [3, 6–9]. This bound can be achieved usually only in the decoherence-free case with the use of collective measurements [11, 12]. Moreover, if we wish to attain the Heisenberg limit, it is usually necessary to use highly entangled states such as NOON states [6, 7, 13, 14], Holland-Burnett states [15], or twin-beam states [16].

In real-life experiments, however, we always have to deal with some sort of decoherence, which can decrease the precision. This issue is especially important for the states used to achieve the Heisenberg limit as these states are often very susceptible to any kind of disturbance. It is known that in the presence of uncorrelated decoherence, when each probe evolves independently from the others, the best possible scaling of precision takes the form of SQL-like scaling $c/\sqrt{\bar{N}}$ [17–19] (with some notable exceptions [10]), where c is a constant, possibly smaller than 1. Although in some cases we can use error-correction [20–22] or fast quantum control [23, 24] techniques to restore the Heisenberg-limited scaling for general decoherence process, the conclusion is that even with entanglement one can only get a constant improvement over the classical SQL scaling.

In this work, we analyze in detail the problem of phase estimation, employing a single-mode bosonic probe evolving in the presence of the most general Gaussian dissipative channel, which, in principle, can be non-Markovian and noncovariant [25]. This general channel involves important physical channels such as lossy or additive noise channels as well as more exotic ones, which involve the evolution of the probe in the presence of a squeezed reservoir. In addition, we also present the results for a closely related problem of frequency estimation for the same setup.

* marcin.jarzyna@fuw.edu.pl

† marcin.zwierz@fuw.edu.pl

Towards the end we give an example of a physical situation in which such an estimation problem may arise.

II. ESTIMATION THEORY

The task of inferring any physical quantity from the experiment is described by quantum estimation theory [26, 27]. A standard quantum parameter estimation setup is depicted in Fig. 1. A probe system prepared in an initial state ρ_0 is sent through a quantum channel Λ_θ . The evolution under this channel results in the output state $\rho_\theta = \Lambda_\theta[\rho_0]$, which depends on an unknown value of the parameter θ we wish to estimate. The output state ρ_θ is then subjected to a general quantum measurement described by a positive operator-valued measure (POVM) $\{\Pi_x\}$. Finally, based on the measurement outcomes x we can calculate the estimated value of the parameter with the help of an estimator function $\tilde{\theta}(x)$. The precision of such an estimation procedure can be quantified with the root-mean-square error $\Delta\theta = [(\langle(\theta - \tilde{\theta}(x))^2\rangle)]^{1/2}$, where the averaging $\langle\bullet\rangle$ is taken with respect to the conditional probability distribution $p(x|\theta) = \text{Tr}[\rho_\theta \Pi_x]$. Note that although the scheme depicted in Fig. 1 is widely used, it is not the most general setup for quantum metrology that one can imagine. A possible extension, created by adding ancillary modes and allowing arbitrary, parameter-independent operations, can also be considered [20–24, 28]; however, here we restrict ourselves to a simple ancilla-free setup.

In order to find the best possible precision one needs to optimize this error over all stages of the estimation procedure, that is, over all possible input states, POVM measurements, and estimator functions. This is, in general, a very hard task. Luckily, the last two optimizations can be avoided by using the quantum Cramér-Rao inequality [26, 29], which states that for every *unbiased* estimator, the estimation error is lower bounded by

$$\Delta\theta \geq \frac{1}{\sqrt{kF_\theta}}, \quad F_\theta = \text{Tr}[\rho_\theta L_\theta^2], \quad (1)$$

where k is a number of independent measurement repetitions, F_θ is the quantum Fisher information (QFI), and L_θ is a Hermitian operator called symmetric logarithmic derivative (SLD), which is defined implicitly via

$$\frac{d\rho_\theta}{d\theta} = \frac{1}{2}(\rho_\theta L_\theta + L_\theta \rho_\theta). \quad (2)$$

The quantum Cramér-Rao bound given in Eq. (1) is known to be saturable in the limit of large number



Figure 1. (Color online) Standard scheme of parameter estimation. A probe system prepared in an initial state ρ_0 is sent through a quantum channel Λ_θ , which depends on an unknown value of the parameter θ we wish to estimate. The output state ρ_θ is then subjected to a general POVM measurement $\{\Pi_x\}$. Finally, based on the measurement outcomes x the value of the parameter is estimated with the help of an estimator function $\tilde{\theta}(x)$.

of repetitions ($k \rightarrow \infty$) with measurements implementing projections on the eigenvectors of the SLD, whose results are processed with the maximum likelihood estimator. The remaining optimization over all possible input states is a much more demanding task as it necessarily involves the knowledge of the exact form of the quantum channel Λ_θ . In many instances one may refer to matrix product states optimization [30] or numerical procedures [31, 32], but still there are some cases that cannot be efficiently solved with those approaches. Another issue is the practicality of the optimal states that can be, in principle, derived from the maximization of the QFI. This is because optimal states are often highly nontrivial in production and therefore it is also important to consider the precision offered by experimentally achievable states, such as, for example, the Gaussian states.

III. EVOLUTION IN THE PRESENCE OF THE MOST GENERAL GAUSSIAN DISSIPATIVE RESERVOIR

We begin our study by introducing the basic ingredients of our parameter estimation procedure. In this paper, we assume that the probe system is prepared in a single-mode bosonic Gaussian state. A general single-mode Gaussian state, which represents probe's initial state, can be written as

$$\rho_0 = D(\alpha_0)S(r_0)\rho_{N_0}S^\dagger(r_0)D^\dagger(\alpha_0), \quad (3)$$

where ρ_{N_0} is a single-mode thermal state with average number of thermal bosons N_0 , $S(r_0) = \exp[\frac{1}{2}(r_0\hat{a}^{\dagger 2} - r_0^*\hat{a}^2)]$ is a squeezing operator and $D(\alpha_0) = \exp[\alpha_0\hat{a}^\dagger - \alpha_0^*\hat{a}]$ is a displacement operator, with \hat{a} and \hat{a}^\dagger being the bosonic annihilation and creation operators. Hence, the class of Gaussian states includes the thermal states, coherent states, and, most importantly, squeezed states (more generally, all states that can be generated with interaction Hamiltonians at most quadratic in \hat{a} and \hat{a}^\dagger belong to this class [33]).

A convenient description of Gaussian states is provided by the phase-space formalism, where any Gaussian state is fully described by only its first and second moments via the Wigner quasiprobability distribution

$$W_0(\mathbf{d}) = \frac{\exp[-\frac{1}{2}(\mathbf{d} - \bar{\mathbf{d}}_0)^\top \Sigma_0^{-1}(\mathbf{d} - \bar{\mathbf{d}}_0)]}{2\pi\sqrt{\det\Sigma_0}}, \quad (4)$$

where $W_0(\mathbf{d})$ is the Wigner function of the initial state ρ_0 , $\mathbf{d} = (x, p)$ is a vector of real eigenvalues of the quadrature position and momentum operators $\hat{x} = 2^{-1/2}(\hat{a} + \hat{a}^\dagger)$ and $\hat{p} = -i2^{-1/2}(\hat{a} - \hat{a}^\dagger)$, with the first moments defined via $\bar{\mathbf{d}}_0 = \langle \hat{\mathbf{d}} \rangle = (\bar{x}_0, \bar{p}_0)$. The second moments $\Sigma_0^{ij} = \frac{1}{2}\langle \hat{\mathbf{d}}_i \hat{\mathbf{d}}_j + \hat{\mathbf{d}}_j \hat{\mathbf{d}}_i \rangle - \langle \hat{\mathbf{d}}_i \rangle \langle \hat{\mathbf{d}}_j \rangle$ are arranged into the covariance matrix Σ_0 . For a general single-mode Gaussian state the covariance matrix, up to phase-space rotations, is given by

$$\Sigma_0 = \left(N_0 + \frac{1}{2}\right) \begin{pmatrix} e^{2r_0} & 0 \\ 0 & e^{-2r_0} \end{pmatrix}. \quad (5)$$

where $H\rho_0 = [a^\dagger a, \rho_0]$ describes a free time-independent unitary evolution of a single bosonic mode a with frequency ω with the superoperators $L[o]\rho_0 = 2o\rho_0 o^\dagger - o^\dagger o \rho_0 - \rho_0 o^\dagger o$ and $D[o]\rho_0 = 2o\rho_0 o - o^2 \rho_0 - \rho_0 o^2$ accounting for a coupling to a squeezed thermal reservoir to which energy is dissipated. Importantly, these superoperators represent also a possible backaction that the reservoir may have on the state of the system [35]. The above master equation takes into account a possible presence of memory effects that may arise from non-Markovian-type evolutions by including explicit time dependence in the coupling strength $\Gamma(t)$. We note that we used the same coupling strength $\Gamma(t)$ for all superoperators, whereas a fully-general non-Markovian master equation may have a different coupling parameter for each of the superoperators [36]; however, this does not affect the generality of our results. The parameters N and M in Eq. (7) are expressed in terms of the average number of thermal bosons N_{th} , the average number of squeezed bosons N_{sq} , and the squeezing angle ξ of the reservoir [34, 35] via

$$N = N_{\text{th}}(2N_{\text{sq}} + 1) + N_{\text{sq}}, \quad (8)$$

$$M = (2N_{\text{th}} + 1)\sqrt{N_{\text{sq}}(N_{\text{sq}} + 1)}e^{i\xi}. \quad (9)$$

These equations are typically combined to provide the relation

$$|M|^2 = N(N + 1) - N_{\text{th}}(N_{\text{th}} + 1), \quad (10)$$

Given the above representation, we can easily calculate the average number of bosons in a single-mode Gaussian state as $\bar{N} = \frac{1}{2}[(N_0 + \frac{1}{2})2\cosh 2r_0 + |\bar{\mathbf{d}}_0|^2 - 1]$.

We consider here a situation in which the probe system prepared in a single-mode Gaussian state ρ_0 evolves under the action of the most general Gaussian dissipative channel. Gaussian evolutions belong to a particularly interesting class of decoherence channels describing many fundamental processes [34, 35], such as lossy or thermal evolutions. The dynamics of ρ_0 evolving under such a channel, in the interaction picture, can be described by the master equation

$$\frac{d\rho_0}{dt} = \mathcal{L}(t)\rho_0, \quad (6)$$

where $\mathcal{L}(t)$ is a *Liouville* superoperator given by

$$\mathcal{L}(t) = -i\omega H + \frac{\Gamma(t)}{2} \{ (N + 1)L[a] + NL[a^\dagger] + M^*D[a] + MD[a^\dagger] \}, \quad (7)$$

which states that N and M are not independent quantities. This fact will become useful in the later analysis.

The formal solution of the master equation in Eq. (6) for time t is given by

$$\rho_\omega = \mathcal{T} \exp \left[\int_0^t \mathcal{L}(s) ds \right] \rho_0 = \Lambda_\omega \rho_0, \quad (11)$$

where \mathcal{T} is the time-ordering operator and the superoperator Λ_ω corresponds to the quantum channel depicted in Fig. 1, with $\theta = \omega$ making this a frequency estimation problem. A quick inspection of Eqs. (7) and (11) shows that we can also write $\rho_\varphi = \Lambda_\varphi \rho_0$, where $\varphi = \omega t$, meaning that this theoretical framework allow us to perform phase estimation as well. Finally, it is important to note that we work here with a tacit assumption of a perfect reference beam accompanying our single-mode probe [37] as estimation employing only a single-mode probe system is not possible.

For a general initial state evolving under a general Gaussian evolution the final parameter-dependent state usually possesses a very complicated form. Fortunately, any Gaussian state undergoing Gaussian evolution remains Gaussian, but its first and second moments are changed [33–35]. The evolution represented by the \mathcal{L} superoperator results in the first moments $\bar{\mathbf{d}} = (\bar{x}, \bar{p})$ for the output state ρ_φ (for the

derivation, see Appendix A),

$$\bar{x} = \sqrt{\eta}(\cos \varphi \bar{x}_0 + \sin \varphi \bar{p}_0), \quad (12)$$

$$\bar{p} = \sqrt{\eta}(-\sin \varphi \bar{x}_0 + \cos \varphi \bar{p}_0), \quad (13)$$

where $\eta = \exp[-\int_0^t \Gamma(s)ds]$ is a *time-dependent* dissipation coefficient. The evolved covariance matrix takes a far more complicated form,

$$\Sigma = \eta(\Sigma_\varphi - \Sigma_N) + \Sigma_N + \Sigma_M, \quad (14)$$

where $\Sigma_N = (N + \frac{1}{2})\mathbb{1}$, $\Sigma_\varphi = R(\varphi)\Sigma_0 R^\top(\varphi)$ is the covariance matrix Σ_0 of the input state rotated by an angle φ [38] and Σ_M is given in Appendix A. The analogous first and second moments can also be written for the output state ρ_ω by replacing φ with ωt .

In summary, we wish to stress that the above results fully describe the evolution of a single-mode Gaussian probe state in the presence of an arbitrary Gaussian dissipative reservoir including the non-Markovian reservoirs.

IV. PRECISION BOUNDS

In order to calculate the precision bounds for phase and frequency estimation we use the expression for the QFI that was derived in Ref. [39]. In that paper, the QFI for any single-mode Gaussian state characterized with the first moments $\bar{\mathbf{d}}$ and the covariance matrix Σ is given by

$$F_\theta = \frac{1}{2} \frac{\text{Tr}[(\Sigma^{-1}\Sigma')^2]}{1 + \mu^2} + \frac{2\mu'^2}{1 - \mu^4} + \bar{\mathbf{d}}'^\top \Sigma^{-1} \bar{\mathbf{d}}', \quad (15)$$

where $\mu = \frac{1}{2}|\Sigma|^{-1/2}$ is the purity and the primed symbols simply represent the corresponding first derivatives with respect to the parameter θ (in our work this parameter is either φ or ω).

Given the above formula and the definitions of the moments in Eqs. (12), (13), and (14), we obtain expressions for the QFIs and the corresponding precision bounds for the phase and frequency estimation in the presence of the most general Gaussian reservoir. Alas, the resulting precision bounds are very complicated and, of course, crucially depend on the input state parameters that we have chosen. Therefore, we present here only the expressions for the asymptotic bounds in the limit of large average number of probes for two types of input states, that is, for the optimal Gaussian state, which happens to be the squeezed-vacuum state and for the coherent state whose performance is usually treated as a benchmark of a classical behavior. The full expression for the QFI for the general Gaussian state is given in Appendix B. We note also that a related problem of estimating parameters of a general Bogoliubov transformation was analyzed in Ref. [40].

A. Phase estimation

An optimization over all single-mode input Gaussian states, that is, an optimization over parameters \bar{x}_0 , \bar{p}_0 , N_0 , and r_0 , reveals that asymptotically, for a large average number of bosons \bar{N} , it is optimal to prepare the probe system in a squeezed-vacuum state. Importantly, unless environmental squeezing vanishes, our channel is not covariant; i.e., the phase shift does not commute with decoherence and therefore unlike most cases analyzed previously in the literature, the QFI *does* depend on the actual value of φ . For simplicity, we assume here that we are interested in estimating the local value of the phase around $\varphi = 0$. This leads to the asymptotic precision bound for phase estimation in the presence of the most general Gaussian dissipative reservoir, which up to the leading order in N , is given by

$$\Delta\varphi \geq \sqrt{\frac{1 - \eta}{4\eta\bar{N}}}(1 + 2N - 2|M|\cos\xi), \quad (16)$$

where $\eta = \exp[-\int_0^T \Gamma(s)ds]$ is the general time-dependent dissipation coefficient with T denoting the total time of the interaction of the probe system with the reservoir. The above result states that as long as $\eta < 1$ or $1 + 2N - 2|M|\cos\xi \neq 0$ we obtain at best an SQL-type scaling with the advantage over the $1/\sqrt{\bar{N}}$ scaling limited to the scaling constant. This suggests that if we were able to tune coefficients N and M in such a way that $1 + 2N - 2|M|\cos\xi = 0$, then the higher-order terms, proportional to $1/\bar{N}$, would become dominant and we would obtain Heisenberg-limit-like scaling of the precision. Unfortunately, we find that such a choice *is not* possible. To see this, let us assume, without loss of generality, that $\xi = 0$ [41], which implies the following condition $|M| = N + \frac{1}{2}$. Combining this condition with Eq. (10) results in an equation for N_{th} that has only one (unphysical) solution: $N_{\text{th}} = -1/2$. If we were permitted to set $|M| = N + \frac{1}{2}$ (which, in fact, is approximately true for an infinitely squeezed dissipative reservoir characterized with $N_{\text{th}} = 0$ and $N_{\text{sq}} \rightarrow \infty$), then the leading order of the asymptotic precision bound would be equal to $\sqrt{1 + \eta^2/4\eta\bar{N}}$, which would represent a far better, Heisenberg-limited precision than the standard optimal result for lossy phase estimation of $\sqrt{(1 - \eta)/4\eta\bar{N}}$ and only a slightly worse than the optimal scaling for the case without dissipation, that is, the case with $\eta = 1$, given by $1/\sqrt{8\bar{N}(\bar{N} + 1)}$ (for details, see Fig. 2) [42].

As the above discussion suggests the most favourable Gaussian dissipative reservoir that we can consider is a *purely squeezed* dissipative reservoir with $\xi = 0$, for which $N_{\text{th}} = 0$ and N_{sq} takes a fixed value. In such a case, Eq. (16) can be rewritten to

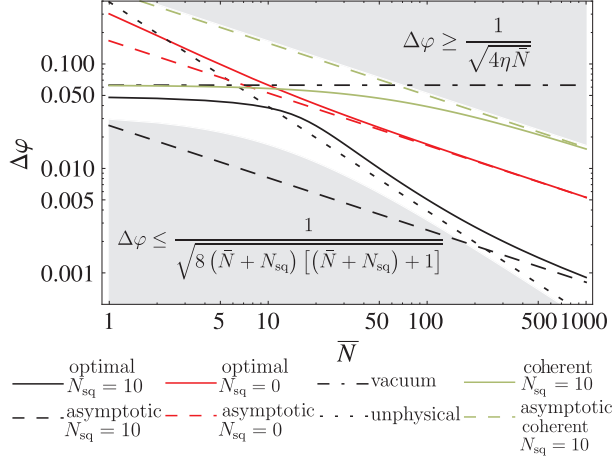


Figure 2. (Color online) The exact precision bound for phase estimation in the presence of a purely squeezed dissipative reservoir with $N_{\text{sq}} = 10$ and $\xi = 0$ (black solid curve) plotted as a function of the average number of input probes \bar{N} for $\eta = e^{-\Gamma T} = 0.9$. The green solid curve is the exact precision bound attainable for an input probe prepared in the coherent state in the presence of our squeezed reservoir, whereas the red solid curve represents the exact precision bound for the standard lossy phase estimation for which $N_{\text{sq}} = 0$. The dashed lines of respective colors are the corresponding asymptotic precision bounds given by Eq. (17) and Eq. (18) (with $N_{\text{sq}} = 0$ for the red dashed line). The horizontal black dash-dotted line depicts the precision obtained for the single-mode vacuum input state for our dissipation model. The black dotted line represents an unphysical Heisenberg scaling of $\sqrt{1 + \eta^2/4\eta\bar{N}}$, which would hold for an infinitely squeezed reservoir. The gray shaded areas represent the precision region lying below the best possible bound of the dissipation-free case (lower one), where for the purpose of a fair comparison we included into the resource count the squeezed bosons of the reservoir as if they were a part of the probe system, and the precision region lying above the sub-SQL-type bound of the standard lossy phase estimation obtained with coherent input states (upper one).

the leading order in \bar{N} as

$$\Delta\varphi \geq \sqrt{\frac{1-\eta}{4\eta\bar{N}}} \left[1 + 2N_{\text{sq}} - 2\sqrt{N_{\text{sq}}(N_{\text{sq}} + 1)} \right], \quad (17)$$

where we set $N = N_{\text{sq}}$ and $|M| = \sqrt{N_{\text{sq}}(N_{\text{sq}} + 1)}$ as per relation (10). In Fig. 2, we plot the above asymptotic precision bound for a realistic value of $N_{\text{sq}} = 10$ [43] (black dashed line) together with the exact precision bound (black solid curve), that is, the precision bound which is numerically optimized for each \bar{N} over all single-mode Gaussian input states. In that figure, we set $\Gamma(s) = \Gamma$. This choice corresponds to the so-called Markovian dissipation model in which $\eta = e^{-\Gamma T}$ represents the usual loss coefficient.

For the purpose of comparison, we further plot the exact (red solid curve) and the asymptotic (red dashed line) precision bounds for the standard lossy phase estimation for which $N_{\text{sq}} = 0$. As expected, the presence of squeezed bosons in the dissipative reservoir, instead of the vacuum, allows for an improved phase estimation for all values of \bar{N} . This improvement is most clearly visible in two regimes. In the regime of small values of \bar{N} , the exact precision bound is flat and lies below that of the standard lossy phase estimation. In this regime, the optimal input state is a single-mode coherent state with a very small admixture of squeezed-vacuum state. In fact, we conclude that for small \bar{N} one can obtain almost optimal performance even if no input bosons are sent into the setup at all (see the horizontal black dash-dotted line in Fig. 2). This behavior is naturally an artifact specific to our dissipation model: The auxiliary squeezed bosons coming from the reservoir encode information about parameter and are used for estimation as well. Furthermore, in the regime of moderate values of \bar{N} , which extends from around 30 to 140 bosons, the error in phase estimation decreases with a Heisenberg-limited fashion. The ratio of the optimal error of our dissipation model to the optimal error of the perfect dissipation-free Heisenberg-limited phase estimation is the smallest for $\bar{N} = 66$ and equal to 1.27.

For the sake of completeness, we finally find that for coherent input states the asymptotically achievable precision, up to the leading order in N , is bounded from below by

$$\Delta\varphi \geq \sqrt{\frac{1 + 2(1-\eta)(N - |M|)}{4\eta\bar{N}}}, \quad (18)$$

where for the sake of simplicity we again assumed $\xi = 0$. This formula indicates that even for coherent input states there exist general Gaussian dissipative reservoirs for which we obtain an improved performance with respect to the standard lossy phase estimation. However, unless the dissipation strength η is small, this improvement is minimal (for details, see Fig. 2). Note also that in the limit $|M| \rightarrow N + 1/2$ the bound converges to the noiseless case $\Delta\varphi \geq 1/\sqrt{4\bar{N}}$, indicating that large environmental squeezing can eliminate the influence of the decoherence.

In summary, we conclude that for an arbitrary Gaussian dissipative evolution the precision in phase estimation is always bounded from below by an SQL-like expression. However, for a range of finite values of \bar{N} , there *always* exist a purely squeezed dissipative reservoir with a fixed value of N_{sq} , which allows us to approach a Heisenberg-limited precision very closely. By increasing the environmental squeezing this range of values becomes proportionally wider

and additionally gets shifted towards larger \bar{N} . Naturally, the above results are also reproduced for fully general Gaussian dissipative reservoirs with $N_{\text{th}} \neq 0$. In the next section, we determine what kind of improvements can be obtained in the case of frequency estimation.

B. Frequency estimation

As we mentioned in Sec. II, the lower bound on the error for frequency estimation is calculated via the quantum Cramér-Rao inequality, Eq. (1). This time, however, the number of independent measurement repetitions k is not arbitrary. This is because, in practice, we fix the total time of the experiment T but we can change time t of each subsequent measurement run. Therefore, the number of repetitions is equal to $k = T/t$ and since we can modify the interrogation time t , the precision of frequency estimation is given by

$$\Delta\omega^2 \geq \frac{1}{kF_\omega} = \min_{0 \leq t \leq T} \frac{t}{TF_\omega}, \quad (19)$$

where the quantum Fisher information for frequency F_ω is calculated from Eq. (15). Therefore, now in order to determine the fundamental precision of frequency estimation we first optimize the quantum Cramér-Rao inequality over all possible input states and then additionally over time t . Analogously to the case of phase estimation, we are interested in estimating the local value of frequency around $\omega = 0$, i.e., the detuning from a known frequency.

Since Eq. (19) explicitly involves optimization over time, the optimal precision will crucially depend on the form of the function $\Gamma(t)$. Here we will focus on a particular class of power functions in the form of $\Gamma(t) = \Gamma t^\beta$, where β is a natural number. This choice is justified since, typically, non-Markovian effects appear on small time scales and then we may expand almost any, even very complicated, function $\Gamma(t)$ around $t = 0$ and consider only its behavior to the leading order. For this reason, this power function is one of the most common choices when considering non-Markovian effects in quantum metrology [44–46]. It is important to note here that the units of proportionality constant Γ depend on the actual value of β , but its value depends on the particular design of the experiment and the nature of decoherence process involved.

Under the above assumption an optimization of Eq. (19) over all single-mode input Gaussian states followed by an optimization over time t leads to an asymptotic precision bound for frequency estimation in the presence of the most general Gaussian dissipative

reservoir,

$$\Delta\omega^2 T = \frac{1}{4} \left[\left(\frac{1+\beta}{2\beta} \right)^\beta \frac{\Gamma(1+2N-2|M|\cos\xi)}{N^{2\beta+1}} \right]^{\frac{1}{\beta+1}}, \quad (20)$$

with the optimal interrogation time for large N given by [47]

$$t_{\text{opt}} = \begin{cases} \frac{1}{\Gamma\sqrt{N(1+2N-2|M|\cos\xi)}} & \text{for } \beta = 0, \\ \left(\frac{1+\beta}{2\beta} \frac{1}{\Gamma(1+2N-2|M|\cos\xi)N} \right)^{\frac{1}{\beta+1}} & \text{for } \beta \geq 1. \end{cases} \quad (21)$$

The above bound is asymptotically saturable with squeezed-vacuum states. Based on the above formulas we can draw similar conclusions as in the case of phase estimation. In particular, for an unphysical infinitely squeezed dissipative reservoir characterized with $N_{\text{th}} = 0$ and $N_{\text{sq}} \rightarrow \infty$, and with the squeezing angle ξ set to zero, which all together implies $|M| = N + \frac{1}{2} = N_{\text{sq}} + \frac{1}{2}$ the leading order of the asymptotic precision bound for frequency estimation

would be equal to $\Delta\omega^2 T = \frac{\Gamma^{\frac{1}{\beta+1}}}{16N^2} \left(\frac{\beta}{1+\beta} \right)^{\frac{1}{\beta+1}} (1 + e^{\frac{2}{\beta}})$

for $\beta > 0$ and $\Delta\omega^2 T = \Gamma \frac{1+e^2}{16N^2}$ for $\beta = 0$ with the optimal interrogation time t_{opt} scaling to the leading

order as $\left(\frac{1+\beta}{\beta\Gamma} \right)^{\frac{1}{\beta+1}}$ in the former case and $1/\Gamma$ in the latter [47]. This would give a Heisenberg-like scaling in estimation error representing a great improvement over the standard scaling for lossy frequency estimation given by Eqs. (20) and (21), with $N = M = 0$. For the sake of completeness, we note that the optimal scaling for the case without dissipation, that is, the case with $\Gamma = 0$, is given by Heisenberg-like scaling expression $\Delta\omega^2 T \geq 1/8T\bar{N}(\bar{N} + 1)$ and is attained for the optimal interrogation time equal to the total time of the experiment $t = T$. This reminds us of a similar conclusion that was obtained for the decoherence-free frequency estimation with the help of Greenberger-Horne-Zeilinger states [48, 49]. Let us also note that a similar scaling of precision as in Eq. (20) was reported in Ref. [46], where the system of N qubits was considered evolving under a non-Markovian *covariant* channel.

As for the probe system prepared in a coherent state, we find an asymptotic precision bound for frequency estimation,

$$\Delta\omega^2 T = \Gamma^{\frac{1}{\beta+1}} \frac{|M| - N}{2\bar{N}} \frac{[1 + (1+\beta)W(g_\beta)]^{\frac{\beta}{\beta+1}}}{(1+\beta)W(g_\beta)}, \quad (22)$$

with the optimal interrogation time given by

$$t_{\text{opt}} = \left[\frac{1}{\Gamma} (1 + (1+\beta)W(g_\beta)) \right]^{\frac{1}{\beta+1}}, \quad (23)$$

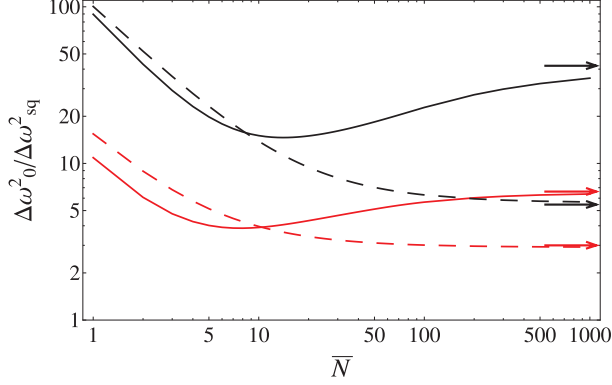


Figure 3. (Color online) The ratio of the exact precision bound $\Delta\omega_0^2$ for the frequency estimation in the case of standard dissipation ($N_{\text{sq}} = N_{\text{th}} = 0$) to the exact precision bound $\Delta\omega_{\text{sq}}^2$ obtained in the presence of a purely squeezed dissipative reservoir ($N_{\text{sq}} = 10$, $N_{\text{th}} = 0$) plotted as a function of the average number of input probes \bar{N} for optimal states with $\beta = 0$ (black solid line) and with $\beta = 1$ (red solid line) and for coherent states with $\beta = 0$ (black dashed line) and with $\beta = 1$ (red dashed line). Arrows of respective colors indicate the asymptotic value of the ratio calculated from Eqs. (20) and (22).

where $W(\bullet)$ is the Lambert W function [50], $g_\beta = \frac{e^{-\frac{1}{\beta+1}}}{1+\beta} \frac{2(|M|-N)}{2(N-|M|)+1}$, and we also assumed that $\xi = 0$. In the simplest case of Markovian evolution with $\beta = 0$, Eqs. (22) and (23) simplify to

$$\Delta\omega^2 T = \frac{\Gamma}{2\bar{N}} \frac{|M| - N}{W(g_0)}, \quad t_{\text{opt}} = \frac{1}{\Gamma} (1 + W(g_0)). \quad (24)$$

This expression represents an improvement over the standard scaling of frequency estimation with coherent states in the presence of loss: $\Delta\omega^2 T = e\Gamma/4\bar{N}$ with the optimal interrogation time given by $t_{\text{opt}} = 1/\Gamma$, as per Eqs. (22) and (23) with $N = M \rightarrow 0$ and $\beta = 0$.

In Fig. 3 we plot the gain in the precision of frequency estimation coming from the squeezing present in the reservoir, which we quantify by the ratio $\Delta\omega_0^2/\Delta\omega_{\text{sq}}^2$ of the precision obtained for the standard dissipation model for a given β to the one obtained with the squeezed reservoir model with the same β . It can be easily seen that the presence of squeezed bosons in the reservoir is advantageous in both the Markovian and the non-Markovian cases for both coherent and optimal states. For optimal Gaussian states the gain is the smallest for moderate average number of input particles \bar{N} and then increases, whereas for coherent states it always decreases. The occurrence of a large gain attainable in the regime of small \bar{N} can be, similarly as in the case of phase estimation, attributed to the presence of squeezed light coming from the reservoir. Addi-

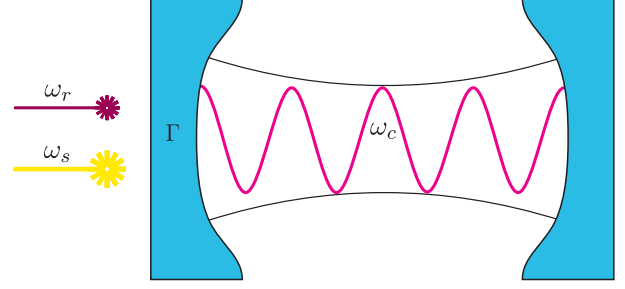


Figure 4. (Color online) Schematic of the effective Fabry-Pérot interferometer. The cavity mode characterized with the resonant frequency ω_c is driven by a coherent driving laser with frequency ω_r and additionally by a broadband squeezed-vacuum light with central frequency ω_s . The effective coupling strength between the coherent and squeezed fields is given by Γ .

tionally, in the non-Markovian case the influence of a squeezed reservoir is weaker when compared to the Markovian one, although we should keep in mind that the asymptotic precision $\Delta\omega^2 T$ in the former case is better than in the latter. In all cases, however, the gain saturates at an asymptotic value larger than 1, indicating that squeezing in the reservoir is beneficial also in the asymptotic regime of large \bar{N} .

Interestingly, the ratio $\Delta\omega_0^2/\Delta\omega_{\text{sq}}^2$ does not depend on the actual value of the coupling strength Γ , although each precision clearly shows a dependence on this parameter. Intuitively, this may be understood by referring to Eq. (19) and observing that a reparametrization of the QFI $F_\omega = t^2 F_{\omega t} = t^2 F_\varphi$ gives us $\Delta\omega^2 T = \min_t \frac{1}{t F_\varphi}$. Since Γ enters the formula for the QFI of phase estimation only through $\eta = \exp[-\Gamma t^{\beta+1}/(1+\beta)]$, we see that the time t always has to fulfill $t \sim \Gamma^{-1/(\beta+1)}$ in order for the exponent to be dimensionless. This, however, means that the dependence on Γ of the precision of frequency estimation is only given through a proportionality constant $\Delta\omega^2 T \sim \Gamma^{1/(\beta+1)}$ irrespective of the presence of squeezed and/or thermal excitations in the reservoir. Therefore, the ratio $\Delta\omega_0^2/\Delta\omega_{\text{sq}}^2$ is the same for all coupling strengths.

V. ESTIMATING THE RESONANCE FREQUENCY OF A CAVITY

So far our study has been purely theoretical. We now wish to convince the reader about the practicality of our ideas. To this end, we present a setup composed of a cavity illuminated by a squeezed beam of light acting as a dissipative reservoir for a coherent laser field [51].

We consider a setup consisting of an effective Fabry-Pérot cavity, which is driven by a stabilized

coherent laser field with frequency ω_r and additionally by a broadband squeezed-vacuum light with central frequency ω_s [51]; the setup is presented in Fig. 4. We wish to sense a detuning $\omega = \omega_c - \omega_r$ of the cavity's resonant frequency ω_c from the coherent laser field frequency by inspecting the light field escaping the cavity at frequency ω_r . The effective coupling strength between the coherent and squeezed fields is given by Γ and we assume that the cavity is *overcoupled*; i.e., the dissipation inside the cavity is negligible as compared to the dissipation characterized by Γ [52]. We further assume the evolution to be Markovian.

Since the input signal beam is in a coherent state we can utilize Eq. (22) to obtain a lower bound on the precision of detuning estimation. Based on the results presented in the previous section we can observe the asymptotic gain $\Delta\omega_{\text{sq}}^2/\Delta\omega_0^2 = \frac{2(|M|-N)}{eW(g_0)}$ in precision resulting from the presence of the environmental squeezing. We observe similar enhancement in precision for all finite values of the average number of photons present in the coherent field (see Fig. 3).

We note that this model describes a situation, where it is fairly easy to change the energy of the (coherent) input beam, while the number of photons in the squeezed beam is fixed. This is very typical for modern quantum-enhanced optical interferometric experiments in which squeezing cannot be arbitrarily high; at the moment, the best sources of squeezed light can produce fields with $N_{\text{sq}} \lesssim 10$ [43, 53, 54]. Finally, let us note that a non-Markovian evolution with $\beta = 1$ is in principle also experimentally feasible in such a model, as shown in [55] [56].

VI. CONCLUSIONS

In conclusion, in the presence of the most general Gaussian dissipative reservoir, even the squeezed

one, the lower bound on the precision of phase estimation always converges to an SQL-like scaling c/\sqrt{N} . However, depending on the type of noise, we can decrease c substantially, especially in the presence of large squeezing in the reservoir (assuming thermal excitations are negligible). This enables us to preserve a Heisenberg-limited precision in the regime of moderate average number of probes, even though asymptotically Heisenberg scaling requires infinite environmental squeezing. Importantly, this advantage is present not only for the optimal Gaussian states, which may be hard to produce experimentally, but also in the case of coherent states. Similar conclusions may be derived for frequency estimation in which one has to additionally optimize the protocol over interrogation time. An interesting open question arising in this context is whether an additional power given to an experimentalist in the form of an error-correction protocol and/or moderate control of the environment would make it possible to preserve Heisenberg-limited scaling also in the regime of finite environmental squeezing. We have also shown that non-Markovian effects, typically appearing on short timescales, influence the precision of frequency estimation. Finally, as exemplified by a toy model presented in the last section, our ideas are not only of theoretical interest but have interesting practical applications.

VII. ACKNOWLEDGMENTS

We thank Rafał Demkowicz-Dobrzański for many insightful discussions and comments on the manuscript. This work was supported by the European Union Seventh Framework Programme (FP7/2007-2013) projects SIQS (Grant Agreement No. 600645; co-financed by the Polish Ministry of Science and Higher Education) and PhoQuS@UW (Grant Agreement No. 316244).

-
- [1] B. P. Abbott *et al.* (LIGO Scientific Collaboration and Virgo Collaboration), Phys. Rev. Lett. **116**, 061102 (2016).
 - [2] B. P. Abbott *et al.* (LIGO Scientific Collaboration and Virgo Collaboration), Phys. Rev. Lett. **116**, 241103 (2016).
 - [3] V. Giovannetti, S. Lloyd, and L. Maccone, Nat. Photon. **5**, 222 (2011).
 - [4] F. Wolfgramm, C. Vitelli, F. A. Beduini, N. Godbout, and M. W. Mitchell, Nat. Photon. **7**, 28 (2012).
 - [5] M. A. Taylor, J. Janousek, V. Daria, J. Knittel, B. Hage, H.-A. Bachor, and W. P. Bowen, Nat. Photon. **7**, 229 (2013).
 - [6] V. Giovannetti, S. Lloyd, and L. Maccone, Phys. Rev. Lett. **96**, 010401 (2006).
 - [7] H. Lee, P. Kok, and J. P. Dowling, Journal of Modern Optics **49**, 2325 (2002).
 - [8] M. J. W. Hall, D. W. Berry, M. Zwiernik, and H. M. Wiseman, Phys. Rev. A **85**, 041802(R) (2012).
 - [9] D. W. Berry and H. M. Wiseman, Phys. Rev. Lett. **85**, 5098 (2000).
 - [10] R. Chaves, J. B. Brask, M. Markiewicz, J. Kołodyński, and A. Acín, Phys. Rev. Lett. **111**, 120401 (2013).
 - [11] K. P. Seshadreesan, P. M. Anisimov, H. Lee, and J. P. Dowling, New J. Phys. **13**, 083026 (2011).

- [12] K. Micadei, D. A. Rowlands, F. A. Pollock, L. C. Céleri, R. M. Serra, and K. Modi, *New J. Phys.* **17**, 023057 (2015).
- [13] I. Afek, O. Ambar, and Y. Silberberg, *Science* **328**, 879 (2010).
- [14] V. Giovannetti, S. Lloyd, and L. Maccone, *Science* **306**, 1330 (2004).
- [15] M. J. Holland and K. Burnett, *Phys. Rev. Lett.* **71**, 1355 (1993).
- [16] P. M. Anisimov, G. M. Raterman, A. Chiruvelli, W. N. Plick, S. D. Huver, H. Lee, and J. P. Dowling, *Phys. Rev. Lett.* **104**, 103602 (2010).
- [17] B. M. Escher, R. L. de Matos Filho, and L. Davidovich, *Nat. Phys.* **7**, 406 (2011).
- [18] R. Demkowicz-Dobrzański, J. Kołodyński, and M. Guță, *Nat. Commun.* **3**, 1063 (2012).
- [19] S. I. Knysh, E. H. Chen, and G. A. Durkin, *arXiv:1402.0495 [quant-ph]* (2014).
- [20] W. Dür, M. Skotiniotis, F. Fröwis, and B. Kraus, *Phys. Rev. Lett.* **112**, 080801 (2014).
- [21] E. M. Kessler, I. Lovchinsky, A. O. Sushkov, and M. D. Lukin, *Phys. Rev. Lett.* **112**, 150802 (2014).
- [22] G. Arrad, Y. Vinkler, D. Aharonov, and A. Retzker, *Phys. Rev. Lett.* **112**, 150801 (2014).
- [23] P. Sekatski, M. Skotiniotis, W. Dür, *New J. Phys.* **18**, 073034 (2016).
- [24] P. Sekatski, M. Skotiniotis, J. Kołodyński, W. Dür, *arXiv:1603.08944 [quant-ph]* (2016).
- [25] A non-covariant channel is a channel in which the unitary part of the evolution does not commute with the part describing decoherence.
- [26] C. W. Helstrom, *Quantum Detection and Estimation Theory* (Academic Press, New York, 1976).
- [27] A. S. Holevo, *Probabilistic and Statistical Aspects of Quantum Theory* (North Holland, Amsterdam, 1982).
- [28] R. Demkowicz-Dobrzański and L. Maccone, *Phys. Rev. Lett.* **113**, 250801 (2014).
- [29] S. L. Braunstein and C. M. Caves, *Phys. Rev. Lett.* **72**, 3439 (1994).
- [30] M. Jarzyna and R. Demkowicz-Dobrzański, *Phys. Rev. Lett.* **110**, 240405 (2013).
- [31] K. Macieszczak, *arXiv:1312.1356 [quant-ph]* (2013).
- [32] M. Jarzyna and R. Demkowicz-Dobrzański, *New J. Phys.* **17**, 013010 (2015).
- [33] S. L. Braunstein and P. van Loock, *Rev. Mod. Phys.* **77**, 513 (2005).
- [34] H.-P. Breuer and F. Petruccione, *The Theory of Open Quantum Systems* (Oxford University Press, Oxford, 2002).
- [35] D. F. Walls and G. J. Milburn, *Quantum Optics* (Springer-Verlag, Berlin, 2008).
- [36] L. Ferialdi, *Phys. Rev. Lett.* **116**, 120402 (2016).
- [37] M. Jarzyna and R. Demkowicz-Dobrzański, *Phys. Rev. A* **85**, 011801(R) (2012).
- [38] C. Weedbrook, S. Pirandola, R. García-Patrón, N. J. Cerf, T. C. Ralph, J. H. Shapiro, and S. Lloyd, *Rev. Mod. Phys.* **84**, 621 (2012).
- [39] O. Pinel, P. Jian, N. Treps, C. Fabre, and D. Braun, *Phys. Rev. A* **88**, 040102(R) (2013).
- [40] N. Friis, M. Skotiniotis, I. Fuentes, and W. Dür, *Phys. Rev. A* **92**, 022106 (2015).
- [41] This is the only suitable choice for ξ as it minimizes the scaling constant of the first sub-SQL-like term in Eq. (16) and, incidentally, results in a squeezed dissipative reservoir that has its squeezing angle aligned with the local value of the phase $\varphi = 0$ to which our setup is calibrated. The importance of this alignment was also pointed out in Ref. [57], where phase estimation in the presence of a squeezed reservoir is studied for the case of the two-level input probe system.
- [42] R. Demkowicz-Dobrzański, M. Jarzyna, and J. Kołodyński, *Prog. Opt.* **60**, 345 (2015).
- [43] J. Aasi *et al.* (The LIGO Scientific Collaboration), *Nat. Photon.* **7**, 613 (2013).
- [44] Y. Matsuzaki, S. C. Benjamin, and J. Fitzsimons, *Phys. Rev. A* **84**, 012103 (2011).
- [45] A. W. Chin, S. F. Huelga, and M. B. Plenio, *Phys. Rev. Lett.* **109**, 233601 (2012).
- [46] A. Smirne, J. Kołodyński, S. F. Huelga, and R. Demkowicz-Dobrzański, *Phys. Rev. Lett.* **116**, 120801 (2016).
- [47] When optimizing t/F_ω , calculated for a squeezed-vacuum state, over t we assume that the optimal time is small in order to simplify the calculation. Following the optimization we expand t_{opt} around $\bar{N} \rightarrow \infty$.
- [48] J. J. Bollinger, W. M. Itano, D. J. Wineland, and D. J. Heinzen, *Phys. Rev. A* **54**, R4649 (1996).
- [49] S. F. Huelga, C. Macchiavello, T. Pellizzari, A. K. Ekert, M. B. Plenio, and J. I. Cirac, *Phys. Rev. Lett.* **79**, 3865 (1997).
- [50] R. M. Corless, G. H. G. H. Gonnet, D. E. G. Hare, D. J. Jeffrey, and D. E. Knuth, *Adv. Comput. Math.* **5**, 329 (1996).
- [51] W. J. Gu, G. X. Li, and Y. P. Yang, *Phys. Rev. A* **88**, 013835 (2013).
- [52] M. Aspelmeyer, T. J. Kippenberg, and F. Marquardt, *Rev. Mod. Phys.* **86**, 1391 (2014).
- [53] J. Abadie *et al.* (LIGO Scientific Collaboration), *Nature Phys.* **7**, 962 (2011).
- [54] H. Yonezawa, D. Nakane, T. A. Wheatley, K. Iwasawa, S. Takeda, H. Arao, K. Ohki, K. Tsumura, D. W. Berry, T. C. Ralph, H. M. Wiseman, E. H. Huntington, and A. Furusawa, *Science* **337**, 1514 (2012).
- [55] K. Jähne, C. Genes, K. Hammerer, M. Wallquist, E. S. Polzik, and P. Zoller, *Phys. Rev. A* **79**, 063819 (2009).
- [56] We note that the non-Markovianity enters our model not through a time-dependent coupling strength $\Gamma(t)$ but rather through time-dependent noise properties of the squeezed reservoir [55].
- [57] S. X. Wu, C. S. Yu, and H. S. Song, *Phys. Lett. A* **379**, 1228 (2015).
- [58] S. M. Barnett and P. M. Radmore, *Methods in Theoretical Quantum Optics* (Oxford University Press, Oxford, 2003).

Appendix A: The moments of the output Gaussian probe state

In order to find the moments for the output state ρ_φ (or alternatively ρ_ω), we transform the master

equation given in Eq. (6) into a Fokker-Planck-type equation for the Wigner function $W_0(\alpha, \alpha^*, t)$ [34, 35, 58]:

$$\begin{aligned} \frac{\partial W_0(\alpha, \alpha^*, t)}{\partial t} = & \left(\frac{\Gamma(t)}{2} + i\omega \right) \frac{\partial}{\partial \alpha} [\alpha W_0(\alpha, \alpha^*, t)] + \left(\frac{\Gamma(t)}{2} - i\omega \right) \frac{\partial}{\partial \alpha^*} [\alpha^* W_0(\alpha, \alpha^*, t)] \\ & + \frac{\Gamma(t)}{2} \left[M \frac{\partial^2}{\partial \alpha^2} + M^* \frac{\partial^2}{\partial \alpha^{*2}} + 2 \left(N + \frac{1}{2} \right) \frac{\partial^2}{\partial \alpha \partial \alpha^*} \right] W_0(\alpha, \alpha^*, t). \end{aligned} \quad (\text{A1})$$

We used here the representation of the Wigner function in terms of the complex amplitudes $\alpha =$

$2^{-1/2}(x+ip)$ and $\alpha^* = 2^{-1/2}(x-ip)$ because it allows us to write the following set of *uncoupled* ordinary differential equations [58]:

$$\begin{aligned} \frac{d}{dt} \langle \alpha^n(t) \alpha^{*m}(t) \rangle = & -n \left(\frac{\Gamma(t)}{2} + i\omega \right) \langle \alpha^n(t) \alpha^{*m}(t) \rangle - m \left(\frac{\Gamma(t)}{2} - i\omega \right) \langle \alpha^n(t) \alpha^{*m}(t) \rangle \\ & + \frac{\Gamma(t)M}{2} n(n-1) \langle \alpha^{n-2}(t) \alpha^{*m}(t) \rangle + \frac{\Gamma(t)M^*}{2} m(m-1) \langle \alpha^n(t) \alpha^{*m-2}(t) \rangle \\ & + \Gamma(t) \left(N + \frac{1}{2} \right) nm \langle \alpha^{n-1}(t) \alpha^{*m-1}(t) \rangle. \end{aligned} \quad (\text{A2})$$

Here the averages are calculated with respect to $W_0(\alpha, \alpha^*, t)$. Based on the above system of equations, we are able to calculate the required moments of $\alpha(t)$ and $\alpha^*(t)$. The formal solutions are given by

$$\langle \alpha(t) \rangle = \sqrt{\eta} \langle \alpha_0 \rangle e^{-i\varphi}, \quad (\text{A3})$$

$$\langle \alpha^*(t) \rangle = \sqrt{\eta} \langle \alpha_0^* \rangle e^{i\varphi}, \quad (\text{A4})$$

$$\langle \alpha^2(t) \rangle = \eta \langle \alpha_0^2 \rangle e^{-2i\varphi} + \eta M C e^{-2i\varphi}, \quad (\text{A5})$$

$$\langle \alpha^{*2}(t) \rangle = \eta \langle \alpha_0^{*2} \rangle e^{2i\varphi} + \eta M^* C^* e^{2i\varphi}, \quad (\text{A6})$$

$$\langle \alpha(t) \alpha^*(t) \rangle = \eta \langle \alpha(0) \alpha^*(0) \rangle + (1 - \eta) \left(N + \frac{1}{2} \right), \quad (\text{A7})$$

where

$$C = \int_0^t \exp \left[\int_0^s \Gamma(\tau) d\tau \right] \Gamma(s) e^{2i\omega s} ds \quad (\text{A8})$$

and $\eta = \exp[-\int_0^t \Gamma(s) ds]$. We can use these solutions to calculate the moments of the quadrature position and momentum operators for the output state

ρ_φ (or alternatively ρ_ω). The first and the second moments (which are arranged into a covariance matrix Σ) are given in the main text in Eqs. (12), (13), and (14). Here we only present a rather complicated form of the Σ_M matrix, which enters the definition of the covariance matrix Σ ,

$$\Sigma_M = \eta |M| |C| \begin{pmatrix} \cos(\theta - 2\varphi) & \sin(\theta - 2\varphi) \\ \sin(\theta - 2\varphi) & -\cos(\theta - 2\varphi) \end{pmatrix}, \quad (\text{A9})$$

where we have defined θ as a phase of MC ; i.e., $MC = |M| |C| e^{i\theta}$.

Appendix B: The exact precision for pure Gaussian states

The exact formula for the QFI of phase estimation with a pure Gaussian probe state evolving under an arbitrary Gaussian evolution characterized by the overall loss coefficient η and parameters N and M is given by

$$\begin{aligned}
F_\varphi = & \frac{4\eta^2(\bar{n} - 2M)^2}{\left\{1 + 2(1 - \eta)(N + M) + 2\eta[\bar{n} + \sqrt{\bar{n}(\bar{n} + 1)}]\right\} \left\{1 + \frac{1}{1 + 4(1 - \eta)(N + M)[(1 - \eta)(N - M) + \eta\bar{n}] + 4\eta(1 - \eta)[N + \bar{n}(N - 1)]}\right\}} + \\
& + \frac{4\eta(\bar{N} - \bar{n})}{1 + 2(1 - \eta)(N - M) - 2\eta[\sqrt{\bar{n}(\bar{n} + 1)} - \bar{n}]}, \tag{B1}
\end{aligned}$$

where \bar{N} is the total average number of photons and $\bar{n} = \sinh^2 r_0$ is the number of squeezed photons in the input state and we have assumed that $\xi = \varphi = 0$ for simplicity. The first part of the above expression is due to the squeezing present in the input, whereas

the second one quantifies the influence of the initial displacement. From Eq. (B1) one can easily obtain the QFI for coherent state input as well as expressions for frequency estimation.